Role of CaMKII and PKA in Early Afterdepolarization of Human Ventricular Myocardium Cell: A Computational Model Study

Dai, L., Zang, Y., Zheng, D., Xia, L. & Gong, Y.

Research Article

Role of CaMKII and PKA in Early Afterdepolarization of Human Ventricular Myocardium Cell: A Computational Model Study

Ling Dai,[1] Yunliang Zang,[1] Dingchang Zheng,[2] Ling Xia,[1] and Yinglan Gong[1]

[1]*Department of Biomedical Engineering, Zhejiang University, Hangzhou, China*
[2]*Health and Wellbeing Academy, Faculty of Medical Science, Anglia Ruskin University, Chelmsford CM1 1SQ, UK*

Correspondence should be addressed to Ling Xia; xialing@zju.edu.cn and Yinglan Gong; yinglangong@zju.edu.cn

Early afterdepolarization (EAD) plays an important role in arrhythmogenesis. Many experimental studies have reported that Ca^{2+}/calmodulin-dependent protein kinase II (CaMKII) and β-adrenergic signaling pathway are two important regulators. In this study, we developed a modified computational model of human ventricular myocyte to investigate the combined role of CaMKII and β-adrenergic signaling pathway on the occurrence of EADs. Our simulation results showed that (1) CaMKII overexpression facilitates EADs through the prolongation of late sodium current's (I_{NaL}) deactivation progress; (2) the combined effect of CaMKII overexpression and activation of β-adrenergic signaling pathway further increases the risk of EADs, where EADs could occur at shorter cycle length (2000 ms versus 4000 ms) and lower rapid delayed rectifier K^+ current (I_{Kr}) blockage (77% versus 85%). In summary, this study computationally demonstrated the combined role of CaMKII and β-adrenergic signaling pathway on the occurrence of EADs, which could be useful for searching for therapy strategies to treat EADs related arrhythmogenesis.

1. Introduction

Early afterdepolarizations (EADs) are triggered before the completion of repolarization [1] and associated with polymorphic ventricular tachyarrhythmia for long QT syndrome patients [2]. Prolongation of action potential duration (APD) and recovery of L-type Ca^{2+} current have been reported as two important factors for the occurrence of EADs [3]. It is also known that the increase of inward currents (e.g., I_{CaL} and late sodium current, I_{NaL}) or the decrease of outward currents (e.g., rapid delayed rectifier K^+ current, I_{Kr} and slow delayed rectifier K^+ current, I_{Ks}) at plateau membrane voltage could increase the probability of EADs events. Therefore, any factors that could change the intensity or time sequence of these currents may lead to the occurrence of EADs [4–8].

Ca^{2+}/calmodulin-dependent protein kinase II (CaMKII) is a key kinase in tuning cardiac excitation-contraction coupling. Its substrates include ion channels, transporters, and accessory proteins [9]. It has been reported that CaMKII phosphorylates I_{CaL}, leading to increased amplitude and

APD prolongation and facilitating the occurrence of EADs [10, 11]. CaMKII can also alter I_{NaL}, transient outward K current (I_{to}), SR Ca^{2+}-ATPase (SERCA) [12], and ryanodine receptor (RyR) channels [10]. It would therefore be useful to understand and quantify these regulatory roles. However, it is very difficult for the laboratory experiments to achieve this. Computer modelling approaches provide alternative ways, allowing us to distinguish the most effective phosphorylation target of arrhythmogenesis, which would ultimately provide useful tool in searching for antiarrhythmia therapy.

It has been known that β-adrenergic signaling pathway regulates Ca^{2+} cycling partly via phosphorylation of I_{CaL} and phospholamban (PLB) [13]. I_{CaL} elevates intracellular Ca^{2+} ($[Ca]_i$) and increases spontaneous Ca^{2+} release via the SERCA inhibition by PLB. The broken balance of Ca^{2+} cycling may contribute to the occurrence of EADs [14–16]. Volders et al. investigated the ionic mechanisms of β-adrenergic on the occurrence of EADs in canine ventricular myocyte and concluded that cellular Ca^{2+} overload and spontaneous SR Ca^{2+} release played important roles in EADs [17].

On the contrary, other studies reported that β-adrenergic agonists activate protein kinase A (PKA), which phosphorylates I_{CaL}, RyR, PLB, SERCA, and I_{Ks}, resulting in delayed afterdepolarization (DADs) [18]. These numerous targets and different temporal characteristics of phosphorylation effects complicate the mechanism analysis of β-adrenergic agonists in relation to EADs. Recently, different computational models have been used to investigate these complex interactions. Xie et al. developed a biophysically detailed rabbit model and found that the faster time course of I_{CaL} versus I_{Ks} increased ISO-induced transient EADs [19] and emphasized the importance of understanding the nonsteady state of kinetics in meditating β-adrenergic-induced EADs and arrhythmia. However, other targets including I_{NaL} have not been investigated thoroughly in their model. It is noted that, although the computational studies of EAD mechanisms have been widely taken, the majority of these published modelling studies have been developed based on nonhuman myocyte. Furthermore, to the best of our knowledge, there is no modelling study considering the combined effect of CaMKII overexpression and β-adrenergic agonists on EADs.

This study aimed to develop a modified computational model of human ventricular myocyte that integrates CaMKII and β-adrenergic signaling networks into a modified ORd's dynamic model [20], with which the combined role of CaMKII and β-adrenergic signaling pathway on the occurrence of EADs would be investigated.

2. Methods

2.1. Integration of CaMKII. Since there is a lack of experimental measurements of human ventricle CaMKII pathway, O'Hara et al. used the Hund-Decker-Rudy's dog model to describe CaMKII kinetics [21, 22]. Our model was developed from the O'Hara-Rudy dynamic model (ORd model) to integrate CaMKII pathway [20]. The following equations describe the CaMKII kinetic of human ventricle:

$$
\text{CaMK}_{\text{bound}} = \text{CaMK}_0 \cdot \frac{1 - \text{CaMK}_{\text{trap}}}{1 + \text{K}_{m\text{CaM}}/\left[\text{Ca}^{2+}\right]_{\text{ss}}},
$$

$$
\text{CaMK}_{\text{active}} = \text{CaMK}_{\text{bound}} + \text{CaMK}_{\text{trap}},
$$

$$
\frac{d\text{CaMK}_{\text{trap}}}{dt} = \alpha_{\text{CaMK}} \cdot \text{CaMK}_{\text{bound}} \cdot \left(\text{CaMK}_{\text{bound}} + \text{CaMK}_{\text{trap}}\right) - \beta_{\text{CaMK}} \cdot \text{CaMK}_{\text{trap}},
$$

(1)

$$
\alpha_{\text{CaMK}} = 0.05 \, \text{ms}^{-1}, \; \beta_{\text{CaMK}} = 0.00068 \, \text{ms}^{-1}, \; \text{CaMK}_0 = 0.05, \; K_{m\text{CaM}} = 0.0015 \, \text{mM}.
$$

The fraction of active CaMKII binding sites at equilibrium state (CaMK_0) was set to 0.05 at the control state. CaMK_0 of 0.12 was used to simulate CaMKII overexpression according to the study from Kohlhaas et al. [23].

2.2. Integration of β-Adrenergic Signaling Networks. The detailed description of β-adrenergic signaling networks could be found from the published study by Soltis and Saucerman [24]. PKA has been reported to phosphorylate I_{CaL}, PLB, troponin I, RyR, myosin binding protein-C, protein phosphates Inhibitor-I [25], and I_{Ks} [24]. I_{CaL}, PLB, and I_{Ks} were the three key factors in this study to model the inotropic effect of β-adrenergic related to potential EADs occurrence. Although the PKA phosphorylation of Na$^+$/K$^+$ ATPase current (I_{NaK}) has been previously described in the computational models [19, 26], its effect was not included in this study partially because there is a lack of direct measurements of I_{NaK} for the normal human ventricle [20]. The phosphorylation by PKA to the three targets (I_{CaL}, PLB, and I_{Ks}) is described as follows:

$$
f_{\text{avail}} = 0.017 \cdot \frac{\text{LCC}_{b\text{PKA}_P}}{\text{fracLCC}_{bp0}} + 0.983, \tag{2}
$$

$$
\text{dss} = \frac{1}{1.0 + \exp\left(-\left(V + v\text{shift}\right)/4.230\right)}, \tag{3}
$$

$$
I_{\text{CaL}} = \left(\overline{I_{\text{CaL}}} \cdot d \cdot \left(1 - \phi_{I_{\text{CaL,CaMK}}}\right)\right.
$$
$$
\cdot \left(f \cdot (1 - n) + f_{\text{Ca}} \cdot n \cdot j_{\text{Ca}}\right) + \overline{I_{\text{CaL,CaMK}}} \cdot d
$$
$$
\cdot \phi_{I_{\text{CaL,CaMK}}} \cdot \left(f_{\text{CaMK}} \cdot (1 - n) + f_{\text{Ca,CaMK}} \cdot n \cdot j_{\text{Ca}}\right)\left.\right)
$$
$$
\cdot f_{\text{avail}}, \tag{4}
$$

$$
\Phi_{I_{\text{CaL,CaMK}}} = \frac{1}{1 + \text{K}m, \text{CaMK}/\text{CaMK}_{\text{active}}}, \tag{5}
$$

$$
td = 1.2 \cdot \left(0.6 \right.
$$
$$
\left. + \frac{1}{\exp\left(-0.05 \cdot (V + 6.0)\right) + \exp\left(0.09 \cdot (V + 14.0)\right)}\right). \tag{6}
$$

Equation (2) shows the coefficient that represents the effect of PKA on I_{CaL} phosphorylation. In (3), the value of "$v$shift" was increased from 3.94 (no ISO application) to 10.0 (for saturated ISO application), which means that the steady state activation curve of I_{CaL} was moved left by 6.06 mV. The permeability of ion Ca^{2+} was increased by 10% with saturated ISO application. Equation (4) describes the augmentation of I_{CaL} amplitude by multiplying "f_{avail}" with the value without PKA phosphorylation, and this represents how PKA regulates

TABLE 1: Current increment and EADs occurrence when different targets were phosphorylated by CaMKII independently.

Cycle length (ms)	I_{Kr} blockage level (%)	CaMKII target (CaMK$_0$ = 0.12)	Target current variation	Deactivation time (ms)	EADs
2000	85	I_{NaL}	Decreased by 24% (from 0.25 to 0.19 $\mu A/\mu F$)	1297 versus 761 ms	Alternated
		I_{CaL}	Increased by 4.2% (from 1.67 to 1.74 $\mu A/\mu F$)		No
		I_{CaK}	Increased by 6.5% (from 0.62 to 0.66 $\mu A/\mu F$)		No
		I_{CaNa}	Increased by 8.1% (from 0.37 to 0.40 $\mu A/\mu F$)		No
		I_{to}	Increased by 3.2% (from 0.95 to 0.98 $\mu A/\mu F$)		No

I_{CaL}. In (6), the time constant of activation gate (td) was extended by 20% with saturated ISO application

$$\text{frac}I_{Ksavail} = 0.49 \cdot \frac{I_{KsPKA_p}}{\text{frac}I_{Ksp0}} + 0.51, \tag{7}$$

$$\text{GKs} = \text{frac}I_{Ksavail} \cdot \text{GKs}, \tag{8}$$

$$Xs05 = 11.60 \cdot \text{frac}I_{Ksavail}, \tag{9}$$

$$X_{S1,\infty} = \frac{1}{1 + \exp\left(-\left(V + Xs05\right)/8.932\right)}. \tag{10}$$

Equation (7) describes the factor of phosphorylation to I_{Ks} by PKA, which was used to alter maximum conductance of I_{Ks} (GKs) in (8). Meanwhile, I_{Ks} state steady activation curve was adjusted by time dependent gate value through the factor "frac$I_{Ksavail}$" in (9) and (10).

2.3. Combination of CaMKII and β-Adrenergic Signaling Networks.

$$f\text{PKA}_{PLB} = \left(\frac{\text{PLB\_PKA}_n}{\text{fracPKA}_{PLB_0}}\right) \cdot \frac{1}{4} + \frac{3}{4}, \tag{11}$$

$$f\text{Jupp} = \frac{1.0}{\left(1.0 + K_{m,CaMK} \cdot \left(f\text{PKA}_{PLB}/\text{CaMK}_{active}\right)\right)}, \tag{12}$$

$$\text{Jup} = (1.0 - f\text{Jupp}) \cdot \text{Jupnp} + f\text{Jupp} \cdot \text{Jupp} - \text{Jleak}. \tag{13}$$

CaMK$_{active}$ that is affected by CaMK$_0$ as shown in (1) would influence I_{CaL} in (4) via the fraction of I_{CaL} channels phosphorylated by CaMKII ($\Phi_{I_{CaL,CaMK}}$). The fraction of SERCAs phosphorylated by CaMKII in (12) was affected by "fPKA$_{PLB}$" and "CaMK$_{active}$", representing the effects of PKA and CaMKII on SERCAs, respectively. As shown in (13), SERCAs were separated into nonphosphorylated populations and CaMKII phosphorylated populations. Therefore, the total Ca^{2+} uptake via SERCAs was adjusted by these two networks simultaneously.

2.4. Simulation Strategy.
In order to determine the potential targets in CaMKII-induced EADs, CaMKII was solely overexpressed by assigning the CaMK$_0$ of 0.12 to specific targets (including I_{NaL}, I_{CaL}, I_{CaK}, I_{NaCa}, and I_{to}), respectively, while β-adrenergic signaling was maintained inactive. Next, CaMKII overexpression was applied with ISO administration. 1 μM ISO was applied in this study to simulate its effect on myocyte action potential and ion currents.

The cycle length of 2000 ms was used in this study since it was closer to normal human beat rhythm than the length of 4000 ms used in the experiments from Guo et al. [27]. In Guo et al.'s work, EADs appeared with I_{Kr} blockage of about 85% [27], which was used for comparison in this study. 500 cycles were performed when the simulation reached steady state. In each individual cycle length, the upper bound of solver step size was set 2 ms.

3. Results

3.1. Effect of CaMKII Overexpression on Ion Currents

3.1.1. Late Sodium Current (I_{NaL}). As shown in Table 1 and Figure 1, with the overexpressed CaMK$_0$ value to I_{NaL} of 0.12 and the normal CaMK$_0$ value of 0.05 to other targets, the alternated EADs occur from our simulation with the cycle length (CL) of 2000 ms and I_{Kr} blockage of 85%.

As shown in Figure 1, I_{NaL} amplitudes alternated with overexpressed CaMK$_0$. In beats with EADs, I_{NaL} amplitude was about 24% smaller (0.19 μA/μF versus 0.25 μA/μF) than these with normal CaMK$_0$ value to I_{NaL} and in beats without EADs, I_{NaL} amplitude was also reduced by 32% (0.17 μA/μF versus 0.25 μA/μF). In Figure 1(d), when EADs occurred, I_{NaL} deactivated, which was about 168% of normal beats (1297 ms versus 773 ms) and about 170% of the control situation in Figure 1(b) (1297 ms versus 761 ms), indicating that overexpressed CaMKII phosphorylation level of I_{NaL} reduces its amplitude and prolongs I_{NaL} deactivation process. Furthermore, the results also indicate that the delayed deactivation of I_{NaL}, rather than its amplitude variation, contributes to the formation of EADs.

3.1.2. L-Type Calcium Current (I_{CaL}). Similarly, as shown in Table 1, with the overexpressed CaMK$_0$ to I_{CaL} of 0.12 and
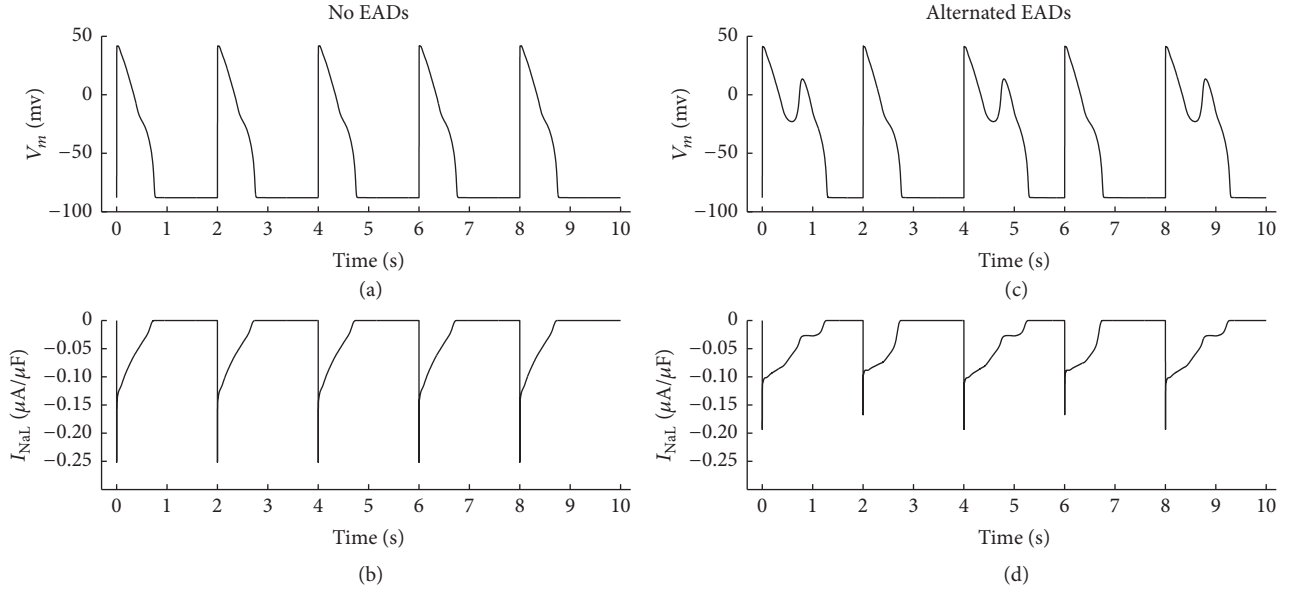
FIGURE 1: (a) No EAD was produced when CaMKII phosphorylation level was in control (CaMK$_0$ = 0.05). (b) Corresponding I_{NaL} when no EADs occurred in (a). (c) Alternated EADs were produced when I_{NaL} phosphorylation by CaMKII was enhanced with CaMK$_0$ of 0.12 and other targets' phosphorylation levels were in control (CaMK$_0$ = 0.05). (d) Corresponding I_{NaL} when alternated EADs occurred in (c). Under these conditions, CL was 2000 ms and I_{Kr} was blocked by 85%.

TABLE 2: Combined effect of CaMKII overexpression and β-adrenergic agonist on EADs.

Cycle length (ms)	ISO application	CaMKII target (CaMK$_0$ = 0.12)	I_{Kr} blockage level (%)	EADs
	None	None	85	None
		None	85	Yes
		None	77	No
2000	1 μM	I_{NaL}	85	Yes
		I_{NaL}	77	Yes
		I_{CaL}	85	Yes
		I_{CaL}	77	No

the normal CaMK$_0$ value of 0.05 to other targets, no EADs occur at CL of 2000 ms and I_{Kr} blockage of 85%, suggesting that the probability of EADs might have little relation with amplitude of I_{CaL}. With the enhanced CaMK$_0$ value to I_{CaL}, the amplitudes of I_{CaL} only increased by 4.2% (1.74 μA/μF versus 1.67 μA/μF).

3.1.3. K$^+$ Current through the L-Type Ca^{2+} Channel (I_{CaK}), Na$^+$ Current through the L-Type Ca^{2+} Channel (I_{CaNa}), and Transient Outward K$^+$ Current (I_{to}). As above, CL was set to 2000 ms and I_{Kr} was blocked by 85%. As shown in Table 1, with enhanced CaMKII phosphorylation level (CaMK$_0$ = 0.12) to different targets, I_{CaK} increased only by 6.5% (0.66 μA/μF versus 0.62 μA/μF), I_{CaNa} by 8.1% (0.40 μA/μF versus 0.37 μA/μF), and I_{to} by 3.2% (0.98 μA/μF versus 0.95 μA/μF). No EADs occurred under all these conditions.

3.2. Combined Effect of CaMKII Overexpression and β-Adrenergic Agonist

3.2.1. Normal CaMKII and 1 μM ISO. The action potentials with different I_{Kr} blockage level are shown in Figure 2. A fixed CL = 2000 ms was used and CaMKII phosphorylation level to all targets was kept control (CaMK$_0$ = 0.05). In Figure 2(a), with I_{Kr} blocked by 85%, stable EADs occurred with the application of ISO, indicating that β-adrenergic agonist facilitates EADs. The I_{Kr} blockage level decreased gradually from 85%, and, when it was decreased to 77%, as shown in Figure 2(b), these EADs disappeared, indicating that 77% was the threshold value for EADs disappearance in this setting. Therefore, 77% was used in following simulation to compare with previously published level of 85% [20]. These results are listed from row 2 to row 3 in Table 2.
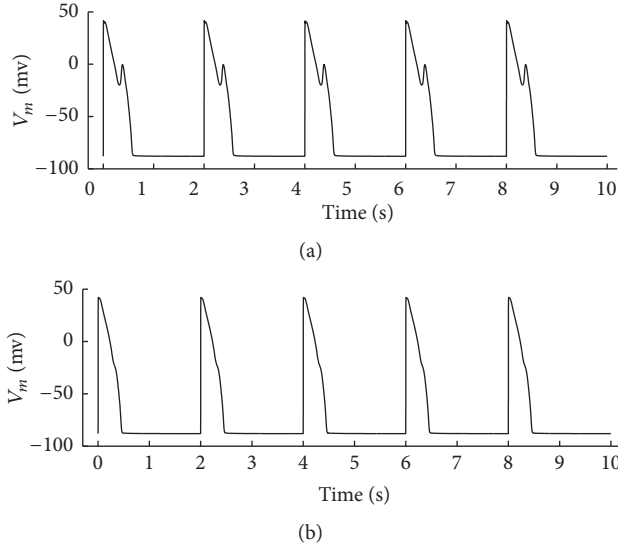
(a)

(b)

FIGURE 2: (a) EADs were induced when $1\,\mu$M ISO was applied and I_{Kr} was blocked by 85%. In (b), EADs disappeared when I_{Kr} blockage was reduced to 77%. Cycle length was set 2000 ms and CaMKII phosphorylation level to all targets was kept control (CaMK$_0$ = 0.05).

3.2.2. Enhanced CaMKII to I_{NaL} and $1\,\mu$M ISO.

As shown in Figure 3, with enhanced CaMKII to I_{NaL} and $1\,\mu$M ISO, when I_{Kr} was blocked by 85%, EADs were induced. The EADs were still observed when I_{Kr} was blocked by 77%, suggesting that I_{NaL} phosphorylation by CaMKII and ISO application together increased the probability of EADs. These results are listed from row 4 to row 5 in Table 2.

3.2.3. Enhanced CaMKII to I_{CaL} and $1\,\mu$M ISO.

As shown in Figure 4, with enhanced CaMKII to I_{CaL} and $1\,\mu$M ISO, when I_{Kr} was blocked by 85%, EADs were induced, but when I_{Kr} blockage was reduced to 77%, EADs disappeared. These results are listed from row 6 to row 7 in Table 2.

4. Discussion

This study developed a modified computational model of human ventricular myocardium cell based on the ORd human model with the integration of regulation mechanism by CaMKII and PKA [20], with which their effects on EADs have been investigated.

EADs often occur during bradycardia under the condition of reduced repolarization reserve. O'Hara's group successfully elicited EADs with cycle length reduced to 4000 ms and I_{Kr} blocked by 85% [20]. In our simulation, with the cycle length halved (2000 ms) and I_{Kr} blocked by 85%, alternated EADs occurred with the sole effect of CaMKII overexpression to I_{NaL}, suggesting that ventricular myocardial cell with CaMKII overexpression is more susceptible to EADs in normal HR range (CL = 2000 ms). Additionally, previous work has shown that I_{CaL} plays an important role in the occurrence of EADs [6]. Our simulation showed that CaMKII overexpression slightly increased I_{CaL} amplitude, but this effect alone did not induce EADs, and CaMKII did not

alter the overlap region of I_{CaL} steady state activation and reactivation curves. Zaza et al. reported that [28], when repolarization is suitably slow, channel reactivation within the overlap region may break the current balance and support the possibility of autoregenerative depolarization. Other inward currents such as Na$^+$-Ca^{2+} exchange current (I_{NaCa}) may play certain roles in triggering EADs if amplitude is augmented and falls into the overlap region. Our simulation results suggest that CaMKII enhances these currents but does not induce EADs via this effect individually. Therefore, when CaMKII is overexpressed, the susceptibility to EADs is mainly originated from I_{NaL} variation.

Our study also demonstrated the behavior of ventricular myocardial cell with the integration of CaMKII overexpression and ISO application. With the ISO application, cyclic AMP (cAMP) is formed through β-adrenergic mediated activation of adenylyl cyclase, which activates PKA, a well-described mediator with targets that promote myocardial performance. In the case where PKA took effect independently, EADs occurred with shorter cycle length (2000 ms versus 4000 ms), indicating that the precondition of EADs is relaxed. Our results were different from that from Xie et al.'s study, where the APD shortening after ISO application was observed without EADs in steady state [19]. Xie et al.'s results could be caused by the simulation of transient I_{CaL} recovery and the prevented spontaneous SR Ca^{2+} release, limiting the I_{NaCa} in forward mode. Therefore, when the cells step into steady state with small inward I_{NaCa}, the shortening of APD could be reasonable. In our work, SR Ca^{2+} release was enhanced by I_{CaL} amplification. With the integration with I_{Kr} blockage, I_{NaCa} was more likely to work as inward current, contributing to the prolongation of APD and occurrence of EADs. Additionally, the shortening of APD was also obtained without I_{Kr} blockage when β-adrenergic pathway was activated. Simulation results showed that when cycle length was chosen at 500 ms, 1000 ms, 1500 ms, 2000 ms, and 4000 ms, the corresponding APD90 shortening was 31.6 ms (233.0 versus 201.4 ms), 30.5 ms (268.6 versus 238.1 ms), 22.3 ms (282.6 versus 260.3 ms), 17.3 ms (289.1 versus 271.8 ms), and 18.6 ms (305.6 versus 287.0 ms). These results were consistent with the experiment measurements from Volders et al. [29]. In the case that CaMKII overexpression acted on I_{NaL} alone with ISO application, EADs occur at CL = 2000 ms and I_{Kr} blockage by 77%, suggesting that the combination of PKA and CaMKII overexpression on I_{NaL} relaxes the precondition further (I_{Kr} blockage 77% versus 85%) and increases the probability of EADs. With the CaMKII overexpressed on I_{CaL} alone, PKA induced EADs occurrence with 85% I_{Kr} blockage, not 77% I_{Kr} blockage, suggesting that, with the ISO application, I_{NaL} phosphorylation by CaMKII has more effect on EADs than I_{CaL}. The steady state of CaMK$_{active}$ was simulated with and without ISO application when CL = 2000 ms, and their corresponding maximum values were 0.0469 and 0.0421, respectively. This suggests that CaMKII activation increased with the application of ISO.

Our simulation results have shown that our proposed model is useful for exploring the interaction of β-adrenergic receptor signaling and CaMKII in formation of EADs; some
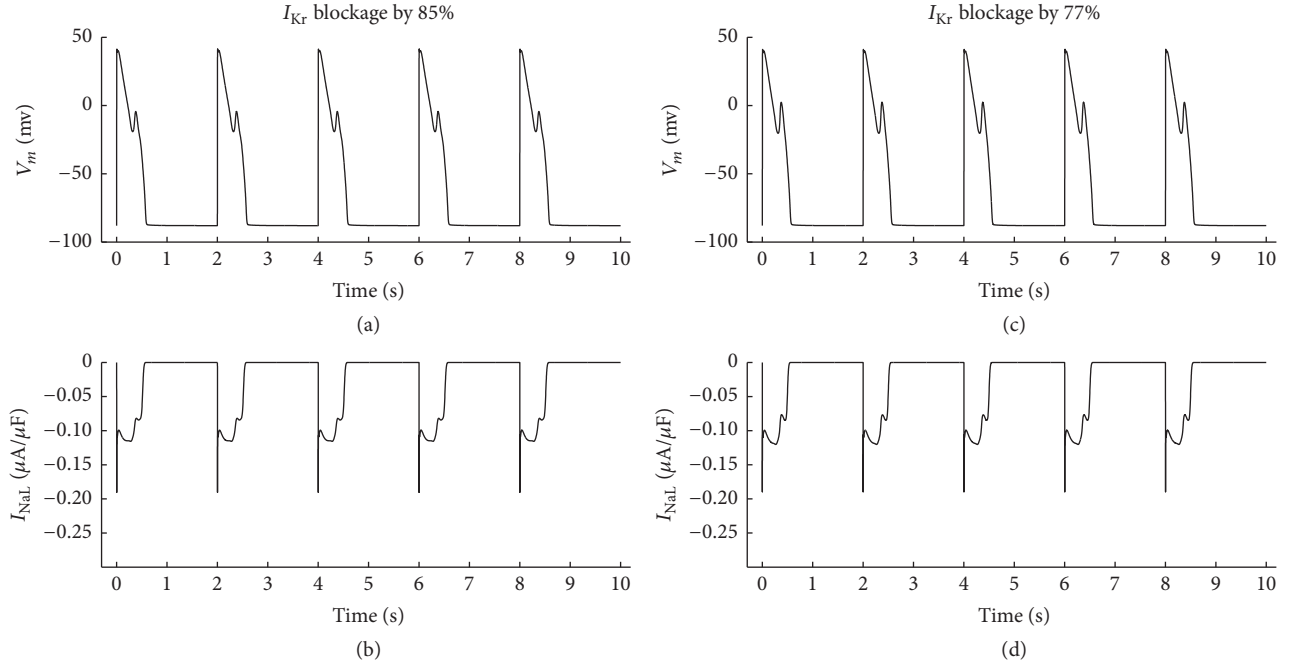
FIGURE 3: EADs occurred when I_{Kr} was blocked by 85% (a) and 77% (c); corresponding I_{NaL} when I_{Kr} was blocked by 85% (b) and 77% (d). CL was set 2000 ms, 1 μM ISO was applied and CaMK$_0$ for I_{NaL} was set 0.12 independently.
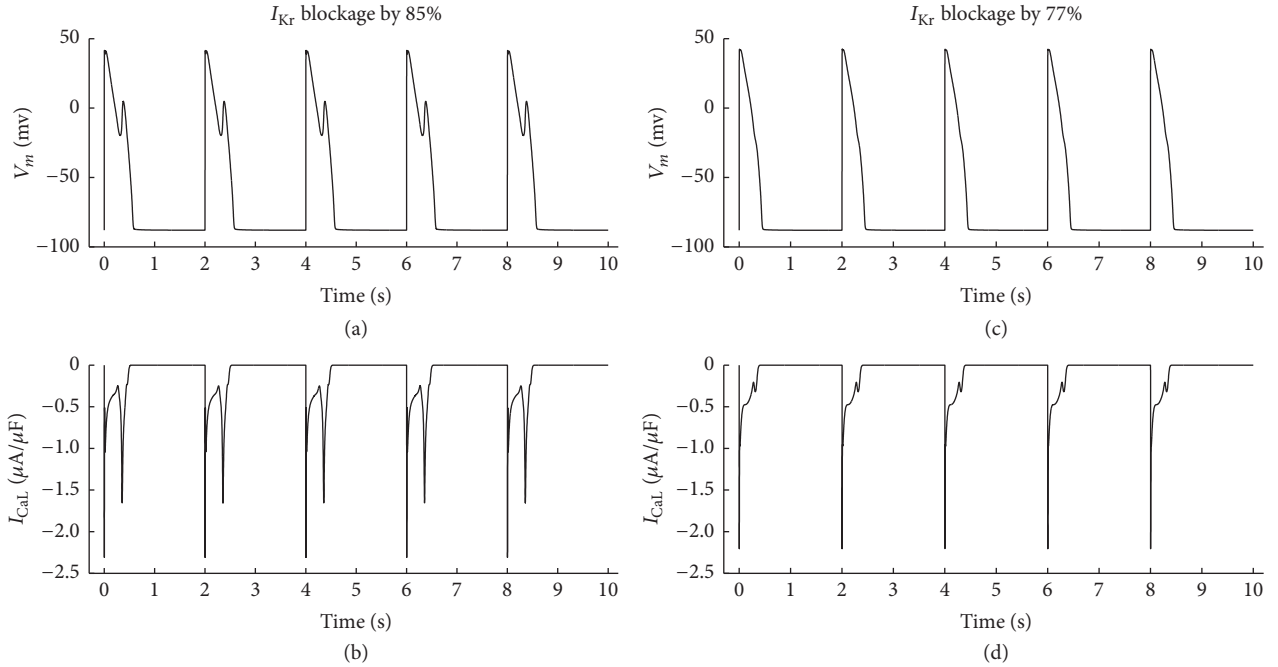

FIGURE 4: 1 μM ISO was applied and cycle length was 2000 ms. CaMK$_0$ for I_{CaL} was 0.12 but CaMK$_0$ for other targets was 0.05. EADs occurred when I_{Kr} was blocked by 85% in (a), but when I_{Kr} blockage was reduced to 77%, EADs vanished in (c). (b) I_{CaL} figures when EADs existed. (d) I_{CaL} figures when EADs vanished.

potential limitations need to be addressed. Firstly, the role of CaMKII on RyR function has not been considered. There is growing evidence about its role in modulating RyR function. Increasing Ca^{2+} leak via RyR would limit SR Ca^{2+} load and disturb Ca^{2+} cycling. This should be incorporated into

an improved model in a future study. Secondly, CaMKII overexpression may downregulate inward rectifier potassium current (I_{K1}) and increase baseline I_{K1} amplitude [30]. We did not include any CaMKII effect on I_{K1} in our model. Thirdly, our model only describes the short-term effect of CaMKII

on different current targets. It has been suggested that short-term and chronic effects of CaMKII are different [30–33]. Short-term (milliseconds to hours) CaMKII overexpression may slow I_{to} inactivation and accelerate recovery, but chronic overexpression may downregulate $I_{to,fast}$ and upregulate $I_{to,slow}$ [34]. Therefore, there is a scope to improve our model by taking chronic effects of CaMKII into consideration in future. Fourthly, there is a lack of an accurate measurement about how ISO regulates I_{NaK} with dynamic calcium change during the beat cycle, although it has been published by Gao et al. [35] that ISO regulated I_{NaK} increased (when calcium is $1.4\,\mu$M) or decreased in pump current (when calcium is $0.15\,\mu$M) depending on the intracellular Ca^{2+} concentrations. In our model the resting calcium concentration was $0.12\,\mu$M and the peak calcium concentration was $1.1\,\mu$M. Similar to the simulation work of Heijman et al. [26], by simply increasing the pump current from 17% to 33%, no significant change of I_{NaK} in triggering EADs (results not shown here) has been observed. However, when the continuous experimental data from human ventricular cells is available, the regulation of ISO on I_{NaK} could be incorporated into the model to reconfirm this nonsignificant effect. Fifthly, it has been reported that local regulation of cAMP and substrate phosphorylation play important roles in β-adrenergic receptor signaling [26, 36–38], so it could be useful to incorporate local control mechanism in a future study. Lastly, there are four CaMKII isoforms ($\alpha, \beta, \gamma, \delta$) with different distributions, kinetics, and roles in physiological and pathological adjustments. Until now, these differences have not been fully understood. Developing a model with detailed CaMKII isoforms information could be useful when experiment data are available.

In conclusion, our simulation results computationally demonstrated a better understanding of the combinational effect of CaMKII and ISO stimulus on the occurrence of EADs in human ventricular myocyte, which may provide useful tool to research therapeutic methods for the treatment of arrhythmia.

Competing Interests

The authors declare that there is no conflict of interests regarding the publication of this paper.

Acknowledgments

References

[1] P. F. Cranefield and R. S. Aronson, *Cardiac Arrhythmias: The Role of Triggered Activity and Other Mechanisms*, Futura Publishing Company, New York, NY, USA, 1988.

[2] J. N. Weiss, A. Garfinkel, H. S. Karagueuzian, P.-S. Chen, and Z. Qu, "Early afterdepolarizations and cardiac arrhythmias," *Heart Rhythm*, vol. 7, no. 12, pp. 1891–1899, 2010.

[3] J. Zeng and Y. Rudy, "Early afterdepolarizations in cardiac myocytes: mechanism and rate dependence," *Biophysical Journal*, vol. 68, no. 3, pp. 949–964, 1995.

[4] C. Antzelevitch, Z.-Q. Sun, Z.-Q. Zhang, and G.-X. Yan, "Cellular and ionic mechanisms underling erythromycin-induced long QT intervals and Torsade de Pointes," *Journal of the American College of Cardiology*, vol. 28, no. 7, pp. 1836–1848, 1997.

[5] W. Shimizu and C. Antzelevitch, "Sodium channel block with mexiletine is effective in reducing dispersion of repolarization and preventing torsade de pointes in LQT2 and LQT3 models of the long-QT syndrome," *Circulation*, vol. 96, no. 6, pp. 2038–2047, 1997.

[6] C. T. January, J. M. Riddle, and J. J. Salata, "A model for early afterdepolarizations: Induction with the Ca^{2+} channel agonist Bay K 8644," *Circulation Research*, vol. 62, no. 3, pp. 563–571, 1988.

[7] C. T. January and J. M. Riddle, "Early afterdepolarizations: mechanism of induction and block. A role for L-type Ca2+ current," *Circulation Research*, vol. 64, no. 5, pp. 977–990, 1989.

[8] R. V. Madhvani, Y. Xie, A. Pantazis et al., "Shaping a new Ca^{2+} conductance to suppress early afterdepolarizations in cardiac myocytes," *The Journal of Physiology*, vol. 589, no. 24, pp. 6081–6092, 2011.

[9] P. J. Mohler and T. J. Hund, "Role of CaMKII in cardiovascular health, disease, and arrhythmia," *Heart Rhythm*, vol. 8, no. 1, pp. 142–144, 2011.

[10] Y. Wu, J. Temple, R. Zhang et al., "Calmodulin kinase II and arrhythmias in a mouse model of cardiac hypertrophy," *Circulation*, vol. 106, no. 10, pp. 1288–1293, 2002.

[11] Y. L. Hashambhoy, J. L. Greenstein, and R. L. Winslow, "Role of CaMKII in RyR leak, EC coupling and action potential duration: a computational model," *Journal of Molecular and Cellular Cardiology*, vol. 49, no. 4, pp. 617–624, 2010.

[12] P. D. Swaminathan, A. Purohit, T. J. Hund, and M. E. Anderson, "Calmodulin-dependent protein kinase II: linking heart failure and arrhythmias," *Circulation Research*, vol. 110, no. 12, pp. 1661–1677, 2012.

[13] D. M. Bers, *Excitation-Contraction Coupling and Cardiac Contractile Force*, Kluwer/Academic Publishers, Boston, Mass, USA, 2nd edition, 2001.

[14] S. C. Verduyn, M. A. Vos, A. P. Gorgels, J. Van der Zande, J. D. M. Leunissen, and H. J. Wellens, "The effect of flunarizine and ryanodine on acquired torsades de pointes arrhythmias in the intact canine heart," *Journal of Cardiovascular Electrophysiology*, vol. 6, no. 3, pp. 189–200, 1995.

[15] L. Carlsson, L. Drews, and G. Duker, "Rhythm anomalies related to delayed repolarization in vivo: Influence of sarcolemmal Ca^{2+} entry and intracellular Ca^{2+} overload," *Journal of Pharmacology and Experimental Therapeutics*, vol. 279, no. 1, pp. 231–239, 1996.

[16] Z. Song, C. Y. Ko, M. Nivala, J. N. Weiss, and Z. Qu, "Complex darly and delayed afterdepolarization dynamics caused by voltage-calcium coupling in cardiac myocytes," *Biophysical Journal*, vol. 108, no. 8, pp. 261A–262A, 2015.

[17] P. G. A. Volders, A. Kulcsár, M. A. Vos et al., "Similarities between early and delayed afterdepolarizations induced by isoproterenol in canine ventricular myocytes," *Cardiovascular Research*, vol. 34, no. 2, pp. 348–359, 1997.

[18] C. T. January and H. A. Fozzard, "Delayed afterdepolarizations in heart muscle: mechanisms and relevance," *Pharmacological Reviews*, vol. 40, no. 3, pp. 219–227, 1988.

[19] Y. Xie, E. Grandi, J. L. Puglisi, D. Sato, and D. M. Bers, "β-Adrenergic stimulation activates early afterdepolarizations

transiently via kinetic mismatch of PKA targets," *Journal of Molecular and Cellular Cardiology*, vol. 58, no. 1, pp. 153–161, 2013.

[20] T. O'Hara, L. Virág, A. Varró, and Y. Rudy, "Simulation of the undiseased human cardiac ventricular action potential: model formulation and experimental validation," *PLoS Computational Biology*, vol. 7, no. 5, Article ID e1002061, 2011.

[21] K. F. Decker, J. Heijman, J. R. Silva, T. J. Hund, and Y. Rudy, "Properties and ionic mechanisms of action potential adaptation, restitution, and accommodation in canine epicardium," *American Journal of Physiology—Heart and Circulatory Physiology*, vol. 296, no. 4, pp. H1017–H1026, 2009.

[22] T. J. Hund and Y. Rudy, "Rate dependence and regulation of action potential and calcium transient in a canine cardiac ventricular cell model," *Circulation*, vol. 110, no. 20, pp. 3168–3174, 2004.

[23] M. Kohlhaas, T. Zhang, T. Seidler et al., "Increased sarcoplasmic reticulum calcium leak but unaltered contractility by acute CaMKII overexpression in isolated rabbit cardiac myocytes," *Circulation Research*, vol. 98, no. 2, pp. 235–244, 2006.

[24] A. R. Soltis and J. J. Saucerman, "Synergy between CaMKII substrates and β-adrenergic signaling in regulation of cardiac myocyte Ca^{2+} handling," *Biophysical Journal*, vol. 99, no. 7, pp. 2038–2047, 2010.

[25] M. J. Lohse, S. Engelhardt, and T. Eschenhagen, "What is the role of β-adrenergic signaling in heart failure?" *Circulation Research*, vol. 93, no. 10, pp. 896–906, 2003.

[26] J. Heijman, P. G. A. Volders, R. L. Westra, and Y. Rudy, "Local control of β-adrenergic stimulation: effects on ventricular myocyte electrophysiology and Ca^{2+}-transient," *Journal of Molecular and Cellular Cardiology*, vol. 50, no. 5, pp. 863–871, 2011.

[27] D. Guo, Q. Liu, T. Liu et al., "Electrophysiological properties of HBI-3000: a new antiarrhythmic agent with multiple-channel blocking properties in human ventricular myocytes," *Journal of Cardiovascular Pharmacology*, vol. 57, no. 1, pp. 79–85, 2011.

[28] A. Zaza, L. Belardinelli, and J. C. Shryock, "Pathophysiology and pharmacology of the cardiac 'late sodium current'," *Pharmacology and Therapeutics*, vol. 119, no. 3, pp. 326–339, 2008.

[29] P. G. A. Volders, M. Stengl, J. M. Van Opstal et al., "Probing the contribution of IKs to canine ventricular repolarization: key role for β-adrenergic receptor stimulation," *Circulation*, vol. 107, no. 21, pp. 2753–2760, 2003.

[30] S. Wagner, E. Hacker, E. Grandi et al., "Ca/calmodulin kinase II differentially modulates potassium currents," *Circulation: Arrhythmia and Electrophysiology*, vol. 2, no. 3, pp. 285–294, 2009.

[31] S. Tessier, P. Karczewski, E.-G. Krause et al., "Regulation of the transient outward K+ current by Ca2+/calmodulin- dependent protein kinases II in human atrial myocytes," *Circulation Research*, vol. 85, no. 9, pp. 810–819, 1999.

[32] O. Colinas, M. Gallego, R. Setién, J. R. López-López, M. T. Pérez-García, and O. Casis, "Differential modulation of Kv4.2 and Kv4.3 channels by calmodulin-dependent protein kinase II in rat cardiac myocytes," *American Journal of Physiology—Heart and Circulatory Physiology*, vol. 291, no. 4, pp. H1978–H1987, 2006.

[33] G. P. Sergeant, S. Ohya, J. A. Reihill et al., "Regulation of K_v4.3 currents by Ca^{2+}/calmodulin-dependent protein kinase II," *American Journal of Physiology—Cell Physiology*, vol. 288, no. 2, pp. C304–C313, 2005.

[34] M. E. Anderson, J. H. Brown, and D. M. Bers, "CaMKII in myocardial hypertrophy and heart failure," *Journal of Molecular and Cellular Cardiology*, vol. 51, no. 4, pp. 468–473, 2011.

[35] J. Gao, R. Wymore, R. T. Wymore et al., "Isoform-specific regulation of the sodium pump by α- and β-adrenergic agonists in the guinea-pig ventricle," *The Journal of Physiology*, vol. 516, no. 2, pp. 377–383, 1999.

[36] V. O. Nikolaev, A. Moshkov, A. R. Lyon et al., "β_2-Adrenergic receptor redistribution in heart failure changes cAMP compartmentation," *Science*, vol. 327, no. 5973, pp. 1653–1657, 2010.

[37] P. T. Wright, V. O. Nikolaev, T. O'Hara et al., "Caveolin-3 regulates compartmentation of cardiomyocyte beta2-adrenergic receptor-mediated cAMP signaling," *Journal of Molecular and Cellular Cardiology*, vol. 67, pp. 38–48, 2014.

[38] R. V. Iancu, S. W. Jones, and R. D. Harvey, "Compartmentation of cAMP signaling in cardiac myocytes: a computational study," *Biophysical Journal*, vol. 92, no. 9, pp. 3317–3331, 2007.

The Scientific
World Journal

Gastroenterology
Research and Practice

MEDIATORS
of
INFLAMMATION

Journal of
Diabetes Research

Disease Markers

Journal of
Immunology Research

International Journal of
Endocrinology

PPAR Research

Hindawi

Submit your manuscripts at
http://www.hindawi.com

BioMed
Research International

Journal of
Ophthalmology

Stem Cells
International

ᵉCAM

Evidence-Based
Complementary and
Alternative Medicine

Journal of
Obesity

Journal of
Oncology

Computational and
Mathematical Methods
in Medicine

Behavioural
Neurology

Parkinson's
Disease

AIDS
Research and Treatment

Oxidative Medicine and
Cellular Longevity